



## Spatio-Temporal Study of Criteria Pollutants in Nigerian City

**L. C. Anyika<sup>1</sup>, C. O. Alisa<sup>1</sup>, A. U. Nkwoada<sup>1\*</sup>, A. I. Opara<sup>2</sup>, E. N. Ejike<sup>1</sup> and G. N. Onuoha<sup>1</sup>**

<sup>1</sup>Department of Chemistry, Federal University of Technology Owerri, P.M.B. 1526, Nigeria.

<sup>2</sup>Department of Geology, Federal University of Technology Owerri, P.M.B. 1526, Nigeria.

### Authors' contributions

This work was carried out in collaboration among all authors. Author LCA managed the experimental analyses of the study. Authors AIO, ENE and GNO supervised and wrote the research study protocol. Authors COA and AUN performed the statistical analysis and wrote the first draft of the manuscript. All authors read and approved the final manuscript.

### Article Information

DOI: 10.9734/AJACR/2020/v6i330160

Editor(s):

(1) Dr. Angélica Machi Lazarin, State University of Maringá, Brazil.

Reviewers:

(1) Ajay Kumar Pandey, India.

(2) Dimple Pruthi, Guru Gobind Singh Indraprastha University, India.

(3) R. Kingsy Grace, Sri Ramakrishna Engineering College, India.

Complete Peer review History: <http://www.sdiarticle4.com/review-history/59196>

**Original Research Article**

**Received 08 May 2020**

**Accepted 13 July 2020**

**Published 29 July 2020**

### ABSTRACT

**Aims:** An investigation of characteristic long term air pollutants known for temporal and spatial behaviors was conducted due to increased pollution scenarios in Nigerian cities as a result of deprived environmental enforcement of statutory obligations.

**Study Design:** One of the worlds' most polluted cities (Onitsha lower basin) in Nigeria was selected for spatio-temporal study of three criteria pollutants combined with GIS and MATLAB alongside associated meteorological conditions during harmattan.

**Methodology:** 72-hourly analyses of the nine different locations having 4 sampling sites and 500 meters apart were done from December to February which generated over 19, 440 experimental data per quarter of each annual study.

**Results:** Upper Iweka/Nitel area recorded the highest concentration of SO<sub>2</sub> pollutant at (94.2 µg/m<sup>3</sup>) due to longer residence times and low wind mixing height. Borromeo hospital showed the least active NO<sub>2</sub> region but converges at points 1 due to North-east wind dissimilar to sampling points 1 having the lowest PM<sub>10</sub> distribution. Measured temperature parameter correlates inversely

\*Corresponding author: Email: chemistryfrontiers@gmail.com;

with relative humidity and precipitation. The GIS spatial representation corresponded to temporal variability of gaseous and particulate pollutants.

**Conclusion:** All sampled areas had AQI above 50; hence the study identified SO<sub>2</sub>, NO<sub>2</sub>, and PM<sub>10</sub> as Primary pollutants of Onitsha lower basin.

**Keywords:** Air quality; GIS; harmattan; MATLAB; seasonal variations; air Pollutants; meteorology.

## 1. INTRODUCTION

Air quality is a serious environmental concern that receives poor attention from the government and non-governmental agencies in certain nations. However, in Nigeria for instance, researchers are continuously raising awareness over the occurrence and extent of pollution [1-2]. Studies have confirmed poor air quality of the prosperous emerging metropolises of Nigeria like Lagos and Kano, but also in commercial hubs like Aba, Port Harcourt, and Onitsha with populations of approximately 1.5 - 5 million. Most awful is the official monitoring of air pollution is rare and global health authorities have particularly singled-out Onitsha's air as predominantly toxic rivaling some polluted cities in China and India [3-5]. Subsequently, the reported impact on fossil fuelled combustion, vehicular exhausts, open burning and industrial emissions varies greatly due to seasonal variations especially in Onitsha basins [6]. Hence, the Harmattan and rainy seasons in Nigeria are key dynamics that influence air pollutants distribution and variation in Onitsha, especially the lower basin. It therefore becomes imperative for scientists to investigate the spatio-temporal variants of certain criteria pollutants around Onitsha lower basins of a bid to comprehend the seasonal influence over air quality and meteorological factors. Among such criteria pollutants are SO<sub>2</sub>, PM<sub>10</sub> and NO<sub>2</sub> that are largely combustion and exhaust based emissions [7].

Then again, Nigeria's economy is inclined towards Chinese economy of '*Pollute first and clean up later*' which implies that Nigerian government lacks the enforced statutory and financial requirements to oversee the invasive consequences of industrialization. The challenge however, is to develop alternative energy or at least apply strategies that mitigates air pollution in a sustainable way from commercial and metropolitan cities [8]. On the contrary, industrial and anthropological activities in the commercial city of Onitsha, Nigeria have continued to increase due to booming urban populations, expansive open burning, and below standard

gasoline sold in the country. Meanwhile, efforts to combat pollution are frustrated by lack of reliable and readily available data [4]. Hence, large scale gathering of pollutant information and database development would support Nigeria's regulatory activities and routine checks, and standard protocols [9]. In this sense, Bakri et al. and co-workers [10] observed that real time measurement of CO gas is one of the best approaches for studying air particulates and pollutants. Another investigation also understood during their study of spatio-temporal analysis of particulate matter inside Saudi Arabia that data acquired from remote sensing provides better understanding to spatial vagaries of atmospheric pollutants [11]. In addition, some authors utilized GIS-based and MATLAB analysis studied PM<sub>2.5</sub>, NOx, SO<sub>2</sub>, and CO emission from industrial stack gas and exposure to population of Beijing and urban management [12-13]. They observed that seasonal variation plays an important role in population exposure levels of pollutants as well as offering real time spatial modelings of air pollutants for urban management. Interestingly, in China, SO<sub>2</sub>, NO<sub>2</sub> and PM<sub>10</sub> are classified as the highest three criteria pollutants. Similarly, it has been noted that GIS are a valuable tool for investigating the spatial pattern of air pollution and its involvement in weather conditions [14]. Consequently SO<sub>2</sub>, NO<sub>2</sub> and PM<sub>10</sub> are characteristic long term air pollutants known for temporal and spatial behaviors due to their physical and chemical attributes that affect air quality [15-16]. Thus, this research work will study the Harmattan temporal and spatial concentrations of SO<sub>2</sub>, NO<sub>2</sub>, and PM<sub>10</sub> in Onitsha Lower basin using nine fixed monitoring locations, and to evaluate their association with air quality and some meteorological parameters.

## 2. MATERIALS AND METHODS

### 2.1 Site Description

Onitsha is the capital city of Anambra state in south eastern regions of Nigeria where the study locality subsists. The study area lies between latitude and longitude coordinates of N06° 07' E006° 47', N06° 07' E006° 48', N06° 08' E006°

46', N06° 08' E006° 47' to N06° 0'9 E006° 47' covering nine locations in Onitsha lower basin. The nine locations were Upper Iweka/Nitel, Mission road/Waterside, Uzodinma street, Port Harcourt road/Niger street, Rest house/GRA, Borromeo hospital, Fegge/Nupe Square, Christ the King College (CKC) and Awada/Oraifite street/ABS-Channel. The detailed description of studied areas with geo-referenced coordinates and maps are also shown in our previous paper by Anyika et al. [6], but also represented differently in the digitized map in Fig. 1.

Particulate and gas measurements were determined using a gas monitor manufactured by

Crowncon Model CE 89/336/EEC obtained from the Environmental Protection Agency of Imo State, Nigeria. Relative humidity, windspeed, and temperature were measured by Windrose environmental meter manufactured by Rumsey Environmental LLC model AE.09605. Also calibration and standardization of equipment were performed as described in our previous publication. Analyses were performed every 72 hour. Each of the nine locations had 4 sampling sites and 500 meters apart. The 72 hourly intervals were done from December 1<sup>st</sup> to March 1<sup>st</sup> which constitutes prime months of Harmattan season. Hence, with 4 points in each of the nine stations gives 36 sampling sites.

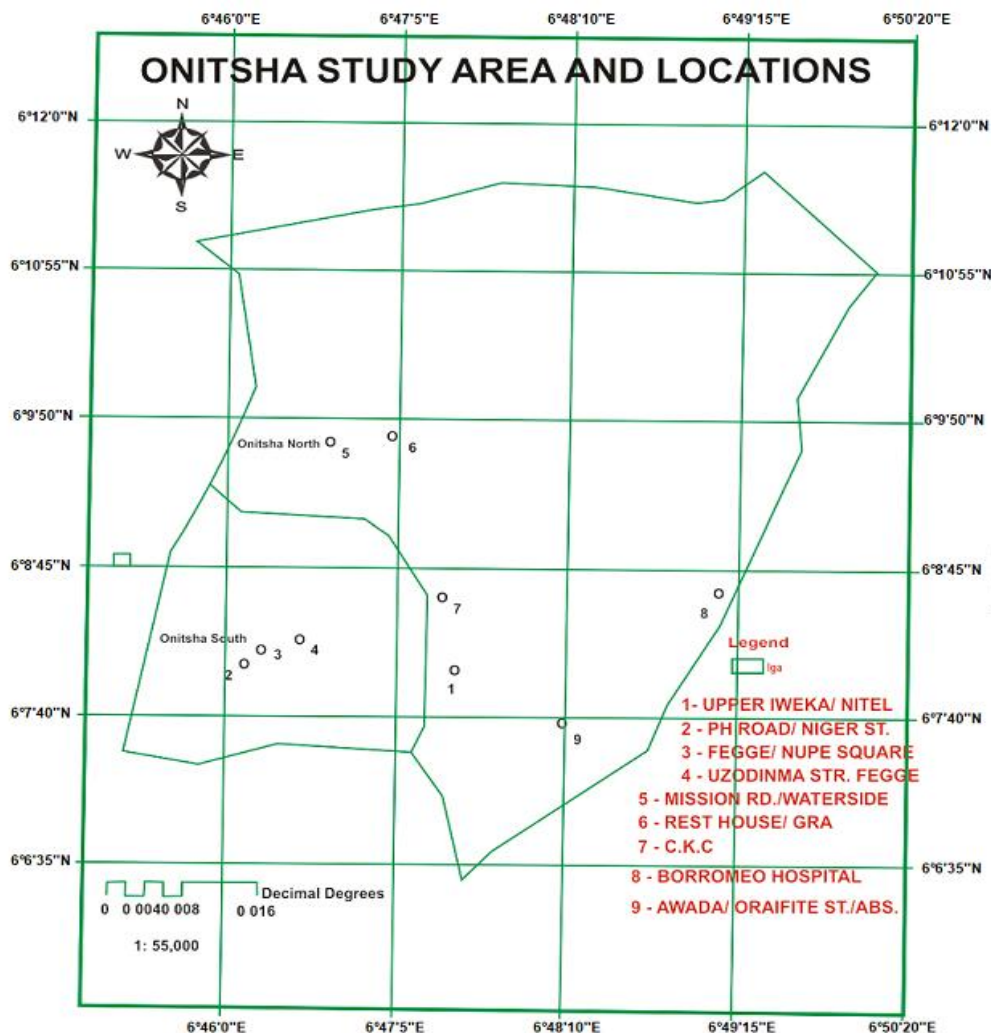


**Fig. 1. Digitized Map of Onitsha study area and locations**  
(Source: Geology Department, FUTO Owerri)

While 6 parameters were measured in each station to give 216 data per day which were averages of three replicates. When measured for 90 days it produces 19, 440 experimental data per quarter of each annual study in 2014 and 2015. The determined values were interpolated to emphasize on sampling points and coordinates rather than monthly variance.

## 2.2 Data Collection and Analysis

GIS/GPS and MATLAB 7.9 software was incorporated into this study and fitted into general finite line models using ARCGIS 9.3 modeling software. The tool enabled calculation of SO<sub>2</sub>, NO<sub>2</sub> and PM<sub>10</sub> concentrations being integrated to evaluate relative humidity, windspeed and temperature peaks. Acquired data with respect to GPS were fitted into ARCGIS 9.3 while MATLAB 7.9 plotted the graph of mean concentrations of weighted coordinates against the nine locations in Onitsha lower basins of Harmattan [14,17,18].

## 2.3 Matlab Modeling

The basis of the model is a mass conversion equation used to simulate dispersion of pollutants from a system of stacks in an industrial cluster as shown below [13, 19]

$$\frac{\partial C^S}{\partial t} = \frac{\partial(U_x C^S)}{d} \quad (1)$$

C<sup>S</sup>= pollutant concentration of the stack  
U = wind speed ("downwind" direction x, m/s)  
s = wind direction.

If the postulation that direction of wind is x, so that bulk transport in this direction exceeds diffusion, then K<sub>x</sub> = 0. Similarly if when no wind velocity exists on Y and Z directions, then equation (1) reduces to

$$\frac{\partial(U_x C^S)}{\partial x} \quad (2)$$

The authors modified the algorithm presented above for solving the rotation matrix [AJ][C] = [D] which results from linearizing equation 2. Here the letter A is taken as a coefficient matrix and C is taken as the concentration matrix, while J is the position angle of elements of matrix A.

The Solution algorithm developed is given below as

- a) Description of domain geometry
- b) Description of meteorological parameters
- c) Description characteristics of each stack
- d) Transformation coordinates and definition of intermediate domain
- e) Solving the finite difference equation in order to get concentrations of each cell domain.
- f) Transformation of results from the opposite direction to get outcomes for the main domain.
- g) Designing of results from two dimensional (2D) and three dimensional (3D)

In both cases atmospheric parameters, transformation of coordinates and solution of partial differential equations as given in equation 1 and 2 must be fulfilled.

## 2.4 Air Quality Index Evaluation

The well-known air quality index (AQI) translates pollution levels in the atmosphere, ranging from 0 to 500. SO<sub>2</sub>, NO<sub>2</sub>, PM<sub>10</sub> criteria pollutants are included in the calculation of the AQI wherein the formula is given below as

$$IAQI_p = \frac{IAQI_{Hi} - IAQI_{Lo}}{BP_{Hi} - BP_{Lo}} (C_p - BP_{Lo}) + IAQI_{Lo} \quad (3)$$

$$AQI = \max (IAQI_1 - IAQI_n) \quad (4)$$

Where IAQI<sub>p</sub> refers to air quality indexes for pollutants, P is per each individual (NO<sub>2</sub>, SO<sub>2</sub> and PM<sub>10</sub>), and Cp is taken as the mean concentration of pollutant P on a daily basis. While BP<sub>Hi</sub> and BP<sub>Lo</sub> identified as the nearby high and low values of C<sub>p</sub>. IAQI<sub>Hi</sub> and IAQI<sub>Lo</sub> refers to air quality indexes in terms of BP<sub>Hi</sub> and BP<sub>Lo</sub> per individual 500 is taking as the highest IAQI value and when the air pollutant's concentration exceeds this highest value, the IAQI<sub>p</sub> is assigned 500 irrespective of IAQI determined. Finally, after determining the value of IAQI<sub>p</sub>, the AQI value is derived by choosing the max IAQI<sub>p</sub> as shown below. More detailed explanation was given in our previous paper [6,19], and studies on Beijing's seasonal variant of atmospheric pollution and air quality [12,19]. Additionally, Table 1 is showing concentration limits for air quality index calculation with high and low values.

**Table 1. Air quality index (AQI) calculation concentration limits**

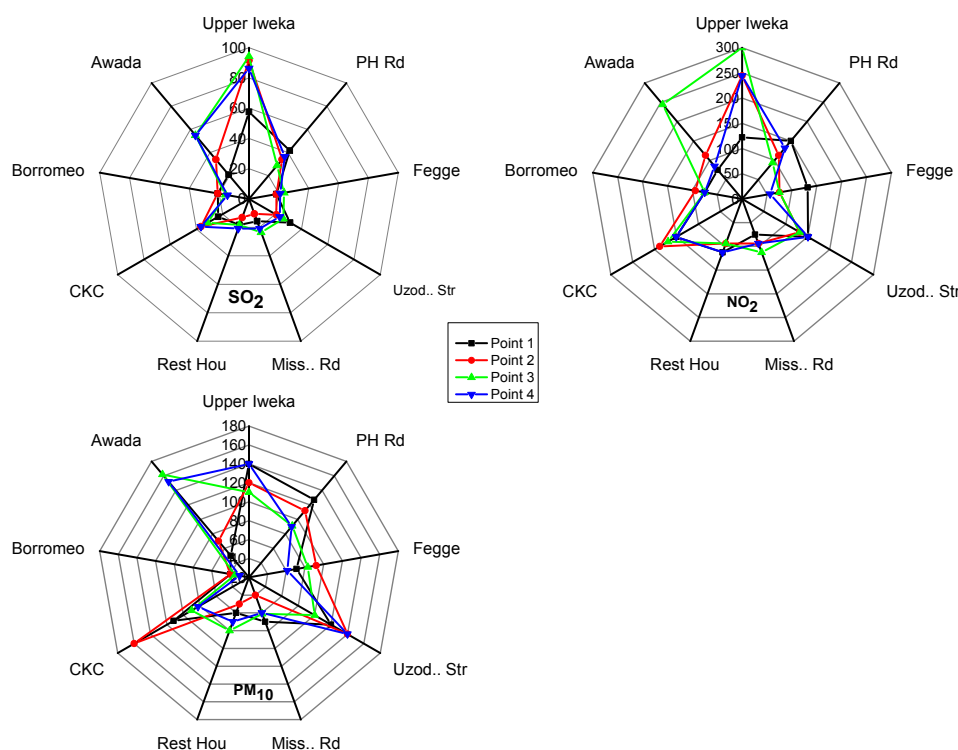
IAQI	PM <sub>10</sub> ( $\mu\text{g}/\text{m}^3$ )	SO <sub>2</sub> ( $\mu\text{g}/\text{m}^3$ )	NO <sub>2</sub> ( $\mu\text{g}/\text{m}^3$ )
50	50	50	40
100	150	150	80
150	250	475	180
200	350	800	280
300	420	1600	565
400	500	2100	750
500	600	2620	940

### 3. RESULTS AND DISCUSSION

#### 3.1 Temporal Variants of SO<sub>2</sub>, NO<sub>2</sub> and PM<sub>10</sub> Concentrations

Determined temporal variations of PM<sub>10</sub>, SO<sub>2</sub> and NO<sub>2</sub> are presented in Fig. 2. The average annual mean of SO<sub>2</sub> ranged from 17-82  $\mu\text{g}/\text{m}^3$ . The graph shows that the upper Iweka/Nitel area recorded the highest concentration of SO<sub>2</sub> pollutant. The least average spread was recorded around mission road/waterside as well as Rest house/GRA. On the other hand, points 1 and 2 were of lower concentrations, while points 3 and 4 presented the most active SO<sub>2</sub> region. The lowest concentration was at Rest

house/GRA (14.4  $\mu\text{g}/\text{m}^3$ ) while the highest SO<sub>2</sub> concentration was at upper Iweka (94.2  $\mu\text{g}/\text{m}^3$ ). The lower trends of SO<sub>2</sub> concentration of other sampling areas may be ascribed to predominance of high winds and rainfall accordingly [14]. While on the contrary, it also indicates that higher concentrations are abundant at less windy areas which encourage accumulation of pollutants. Moreover from the graph, the peak concentration of SO<sub>2</sub> is seen around Upper Iweka, then Awada area while Borromeo area and Fegge presented the lowest dip in concentration. Comparing the experimental results from FEPA (Federal Environmental Protection Agency), Nigeria [20].

**Fig. 2. Radar distribution of SO<sub>2</sub>, NO<sub>2</sub> and PM<sub>10</sub> criteria pollutants**

and NAAQS (National Ambient Air Quality Standard) for ambient air shows that most of the areas were below  $50.0 \mu\text{g}/\text{m}^3$  of FEPA and way below  $25,000 \mu\text{g}/\text{m}^3$  of NAAQS. However, all sampling points in Upper Iweka exceeded FEPA standard while points 3 and 4 of Awada/Oraifite were  $54.9$  and  $55.0 \mu\text{g}/\text{m}^3$  respectively. In addition, WHO annual mean of  $50.0 \mu\text{g}/\text{m}^3$  was exceeded at Upper Iweka and Awada while most sampling was higher than WHO  $20.0 \mu\text{g}/\text{m}^3$  for 24 hr period. The higher concentrations of  $\text{SO}_2$  at Upper Iweka and Awada suggest extended dawdle times of these pollutants due to quiescent conditions and low mixing height [21]. Also being at residential sites, it will be emissions coming from burning of coal and biomass [22]. Secondly, with the growing number of populace desirous of improved residential homes and higher standards of living, the number of licensed motor vehicles in the town increases with corresponding increased emission levels [5]. Subsequently, the emission origins of  $\text{SO}_2$  pollution are categorized as both anthropogenic and non-anthropogenic sources, with the anthropogenic sources estimated to account for more than 70 % of  $\text{SO}_2$  worldwide emissions. Hence, the results strongly suggest that  $\text{SO}_2$  concentrations were mainly due to anthropogenic activities and also responsible for air quality variations [23].

The temporal distribution of  $\text{NO}_2$  pollutant is also presented in Fig.2 radar plot distribution. The average annual mean concentrations of  $\text{NO}_2$  at the sampling sites ranges from  $84.6 \mu\text{g}/\text{m}^3$  at Fegge/Nupe Square to  $227.9 \mu\text{g}/\text{m}^3$  at Upper Iweka/Nitel area. On the other hand, the average  $\text{NO}_2$  concentration was the highest at point 3 ( $244.4 \mu\text{g}/\text{m}^3$ ) and lowest at point 1 ( $75.2 \mu\text{g}/\text{m}^3$ ). The lowest determined concentration was  $56.4 \mu\text{g}/\text{m}^3$  at point 4 of Fegge/Nupe sampling sites while the highest determined concentration was  $300 \mu\text{g}/\text{m}^3$  at point 3 in Upper Iweka. Hence this confirms that  $\text{NO}_2$  pollutant is dominant and dynamic in upper Iweka during Harmattan than other regions, while Borromeo showed the least active  $\text{NO}_2$  region during Harmattan seasons of 2014 and 2015 as seen in Fig.2. Also Upper Iweka, C.K.C area and Awada/Oraifite sampling sites peaked at points 3 sampling stations while PH road/Niger Street and Uzodinma Street and Fegge/Nupe square similarly peaked at points 1. A closer observation of Fig.1 shows that this three sampling areas lie along latitude  $6^{\circ} 46' 0''\text{E}$  and  $6^{\circ} 47' 5''\text{E}$  and longitude  $6^{\circ} 8' 45''\text{N}$  and  $6^{\circ} 7' 40''\text{N}$ . Thus, North-east wind might be driving the  $\text{NO}_2$  pollutant significantly to converge at points

1. The FEPA (stationary sources) standard of  $\text{NO}_2$  is  $75000 \mu\text{g}/\text{m}^3$ , while NAAQS is  $1000 \mu\text{g}/\text{m}^3$  and both are way above the highest determined value of  $300 \mu\text{g}/\text{m}^3$  confirmed in upper Iweka. Although, WHO standard of one hour guideline is  $200 \mu\text{g}/\text{m}^3$ , it however suggests that Upper Iweka is  $\text{NO}_2$  contaminated region. On the other hand, when  $40.0 \mu\text{g}/\text{m}^3$  of WHO annual mean concentration levels where compared to our current data onto Harmattan and previous studies during rains, it depicts that all the sampled area exceeded this value and are therefore heavily polluted by  $\text{NO}_2$  on annual bases [6, 11, 20]. A significant contributor of  $\text{NO}_2$  in this study is the frequent movements of heavy duty diesel trucks along the studied area especially at upper Iweka via vehicles exhaust [24]. The higher concentration of  $\text{NO}_2$  at upper Iweka shows that the pollutant is related to increase from coal and biomass during Harmattan [15]. This also correlates to  $\text{SO}_2$  pattern of distribution and similarly shows that lower  $\text{NO}_2$  distribution at Fegge/Nupe square is due to prevalent high wind speeds and precipitation [14]. Another significant contributor of  $\text{NO}_2$  are the industrial activities centered on upper Iweka, has been similarly observed [25,26]. Moreover, the distance from the monitoring site might equally affect the density of  $\text{NO}_2$  concentration per unit area [22]. In the end, the findings strongly categorize Onitsha lower basin as  $\text{NO}_2$  polluted area having exceeded an annual average guideline value of  $40.0 \mu\text{g}/\text{m}^3$  set by WHO [27].

The temporal data onto  $\text{PM}_{10}$  concentrations are presented below in Fig. 2 showing  $\text{PM}_{10}$  distribution of the sampled area. Average annual concentration of each location ranged from  $65.0 \mu\text{g}/\text{m}^3$  at Rest House to  $127.5 \mu\text{g}/\text{m}^3$  at Upper Iweka. Then again, the average annual concentration of each sampling station ranged from  $87.7 \mu\text{g}/\text{m}^3$  at point 1 to  $91.5 \mu\text{g}/\text{m}^3$  at sampling point 2 for all locations. The Highest concentration measured for  $\text{PM}_{10}$  was  $160$  and  $162 \mu\text{g}/\text{m}^3$  at C.K.C and Awada respectively. While the lowest concentration measured was at Borromeo hospital. A clear observation of Fig. 2 shows that Borromeo hospital had an even spread of the lowest concentrations across the four different sampling points. This might be because a major hospital at Borromeo generates modest  $\text{PM}_{10}$  into the atmosphere. Upper Iweka had the highest spread of  $\text{PM}_{10}$  concentrations that peaked at point 1 and point 4 unlike Awada with uneven distribution of  $\text{PM}_{10}$  across board. The next maximum value determined was  $140$

$\mu\text{g}/\text{m}^3$  at upper Iweka points 1 and 4, while Uzodinma street also recorded  $140 \mu\text{g}/\text{m}^3$  at points 4. FEPA permissible limit value is  $25000 \mu\text{g}/\text{m}^3$ , and when compared to experimental data showed that all the sampling points were below maximum permissible limits. However, for NAAQS of  $150 \mu\text{g}/\text{m}^3$ , only Awada (points 3 and 4;  $162$  and  $152 \mu\text{g}/\text{m}^3$  respectively) and C.K.C at point 2 ( $160 \mu\text{g}/\text{m}^3$ ) exceeded the standard permissible limit. Hence, this similarly confirmed point 1 sampling points to have the lowest  $\text{PM}_{10}$  distribution or least  $\text{PM}_{10}$  polluted sampling spots. Moreover, point 3 showed the highest  $\text{PM}_{10}$  distribution or most polluted sampled spots [6, 11].

Remarkably, the 24-hr average indoor  $\text{PM}_{10}$  value of World Health Organization (WHO) guidelines ( $50.0 \mu\text{g}/\text{m}^3$ ) was exceeded by all locations except at Borromeo in all sampling points [27]. Therefore, it indicated that  $\text{PM}_{10}$  is a major pollutant contributing the most to air quality impact on the studied pollutants in Onitsha Lower basin. This particulate emission of coarse particles when higher than WHO standard possess health problems on the upper and lower respiratory infection, induce cardiovascular disease as well as chronic pulmonary disease. Hence, the residents of Awada, Upper Iweka and CKC may be experiencing outdoor infiltration by  $\text{PM}_{10}$  from vents, windows and doors [28]. Moreover, based on the findings, Upper Iweka in the next decade may be experiencing a more severe  $\text{PM}_{10}$  contamination due to its faster urbanization when compared with the other locations having similar topographic and meteorological conditions [16].

Interestingly, from Fig. 1, it would be observed that Borromeo, Rest House and mission road had correlated with the average lowest distribution of  $\text{PM}_{10}$ ,  $\text{SO}_2$  and  $\text{NO}_2$  in all locations and sampling points as was equally observed [15]. This may also suggest that  $\text{PM}_{10}$  is less distributed at higher altitudes. However,  $\text{SO}_2$  and  $\text{NO}_2$  highest value correlated at Upper Iweka and closely followed by Awada. Coincidentally, Awada had the highest  $\text{PM}_{10}$  concentration and closely followed by C.K.C. This, in the same way, suggests that  $\text{PM}_{10}$  is heavily distributed at lower altitudes. This in-fact is applicable because at lower altitudes air density is higher. Besides, it suggests that the presence of  $\text{SO}_2$  and  $\text{NO}_2$  are playing potential roles in the formation of  $\text{PM}_{10}$  pollutants [23]. Also, some other potential contributors of  $\text{PM}_{10}$  pollutants may include coal combustion, traffic sources and wind-blown road

dust. Other sources might be via commercial activities and the emissions from vehicles, which use diesel oil and probably transported by strong winds [16]. Furthermore, the chemical compositions of  $\text{PM}_{10}$  differ from  $\text{NO}_2$  and  $\text{SO}_2$ , and for that reason, differ with their reaction properties, emission diffusion time and disintegration ability [29].

### 3.2 Spatial Variants of $\text{SO}_2$ , $\text{NO}_2$ and $\text{PM}_{10}$ Pollutants

Measured spatial distribution of  $\text{SO}_2$ ,  $\text{PM}_{10}$  and  $\text{NO}_2$  are represented in the GIS plot below. For illustrative purposes, the pollution pattern of the three criteria pollutants for points 1 is shown in Fig. 3 below. For  $\text{SO}_2$ , it shows that Upper Iweka is the most pollution intense location. This may be due to different pollutant sources of the Upper Iweka area. Also it shows no significant difference in Rest house, Mission road, Fegge/NUPE square, Borromeo and CKC sampling locations and may be affected by meteorological conditions or the  $\text{SO}_2$  emissions does not originate from these sampling areas. While Awada/Oraifite, Uzodinma Street, PH road/Niger Street and Upper Iweka were pollutant receiving areas from active zones.

Observation from  $\text{NO}_2$  GIS plot against Fig. 3(b) reveals that C.K.C, PH road and Uzodinma Street were pollution active centers. Moreover,  $\text{NO}_2$  pollutants appear to emanate from them and spread out towards Upper Iweka, Fegge, and Awada area. Borromeo, Rest house and Mission road were least pollutant active areas and showed no significant difference among. Besides, it confirms that  $\text{NO}_2$  did not originate from these aforementioned sampling areas.

The  $\text{PM}_{10}$  GIS plot of Fig. 3(c) had Upper Iweka, PH road as the most significantly active region with  $\text{PM}_{10}$  pollutants spreading out from these sampling areas. Uzodinma street, Fegge/Nupe square, and Awada/Oraifite were pollutant receiving areas from active regions. While Borromeo, Rest house, Mission road may be affected by other factors and showed no significant difference. This may be due to the influence of meteorological parameters and also indicates that  $\text{PM}_{10}$  pollutant sources were not from them.

They GIS results discussed above are in consonants with temporal variation of respective criteria pollutants. It will be recalled that the highest concentration of  $\text{SO}_2$  was  $91.6 \mu\text{g}/\text{m}^3$  at

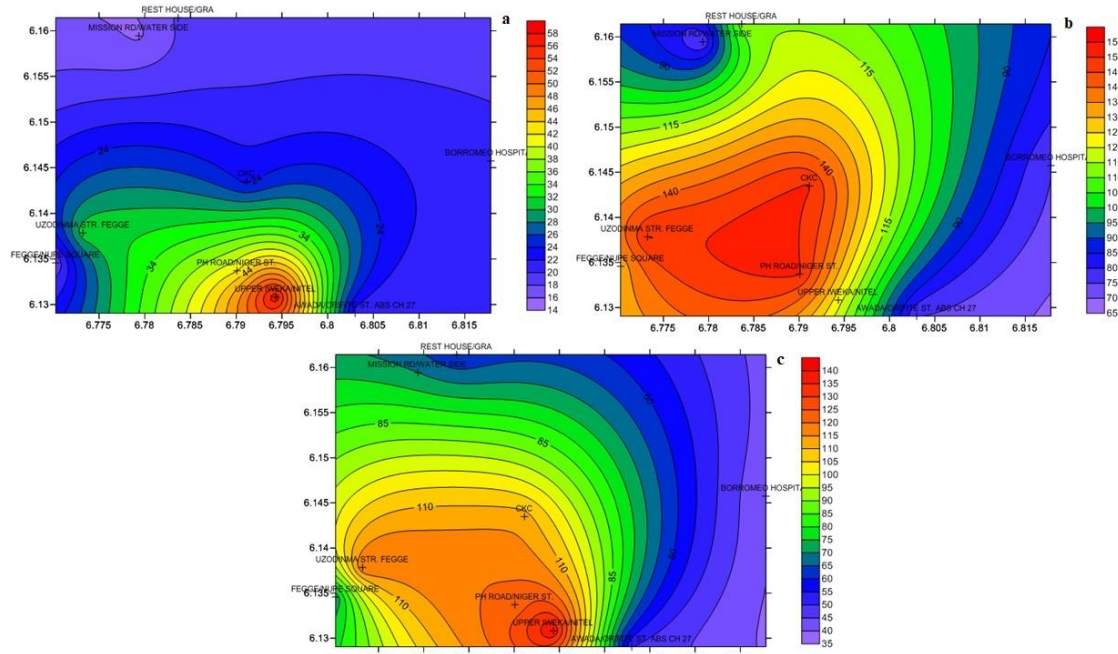
point 2 of Upper Iweka and least value was  $13.1 \mu\text{g}/\text{m}^3$  in point 2 at Rest house. For  $\text{NO}_2$ , it was point 3 ( $300 \mu\text{g}/\text{m}^3$ ) that gave highest concentration while point 1 of Awada, Borromeo and Mission road each had  $75.2 \mu\text{g}/\text{m}^3$ . The  $\text{PM}_{10}$  remarkably was highest at Awada/Oraifite ( $160 \mu\text{g}/\text{m}^3$ ) while Borromeo had a good distribution of low concentration of  $\text{PM}_{10}$  with  $30.0 \mu\text{g}/\text{m}^3$  at point 4. Hence this showed the variations and distributions of  $\text{NO}_2$ ,  $\text{SO}_2$  and  $\text{PM}_{10}$  with Onitsha lower basin during Harmattan at points 1. Interestingly, the GIS spatial representation corresponded to temporal variability of gaseous and particulate pollutants.

### 3.3 Influence of Meteorological Parameters

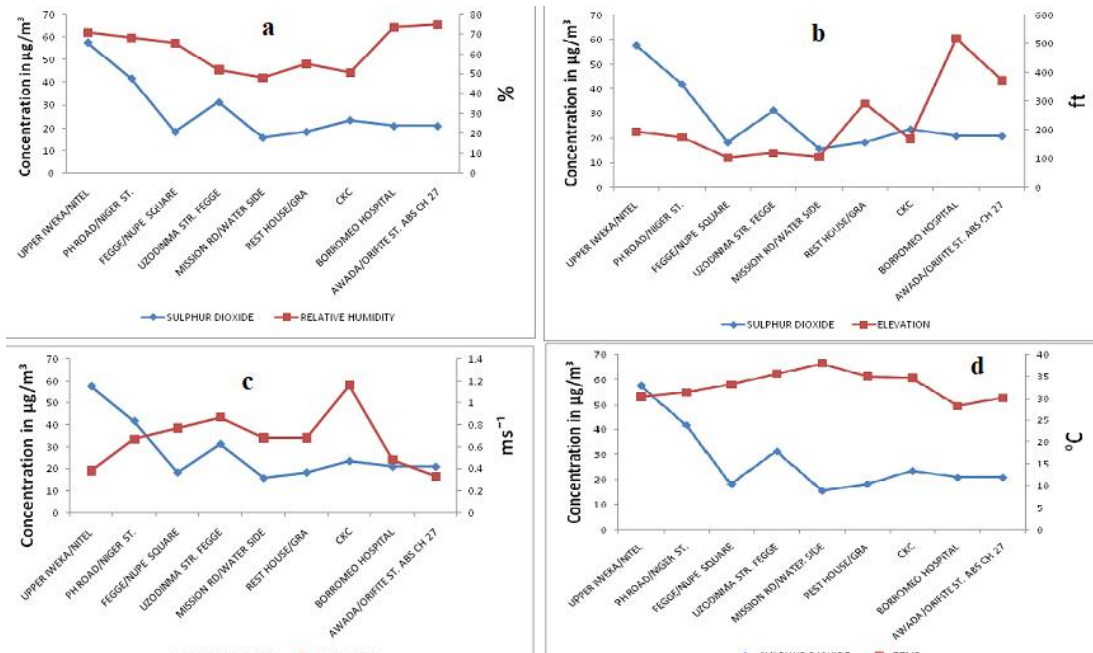
The influence of meteorology was also determined to understand their effects on spatio-temporal behavior of  $\text{SO}_2$ ,  $\text{NO}_2$  and  $\text{PM}_{10}$  gaseous and particulate pollutants over the study area. Fig. 4 shows the graphical inter-relationship for  $\text{SO}_2$  at points 1 sampling stations herein discussed as a reference study.

Fig. 4(a) refers to the relative humidity of the studied area ranging from 50 - 75 %. Relative humidity appears to show very little influence

over the  $\text{SO}_2$  pollutant, suggesting that combined meteorological effects of relative humidity and some other parameters might be a key player rather than a pollutant relationship. On the other hand, at Fig. 4(b) low elevation appears to drive concentration of pollutants higher while higher elevation at CKC, Borromeo and Awada drives a lower concentration. The findings correlated with authors that identified that top urban elevations are responsible for inhibitory effect on urban AQI with consequent improved urban air quality [30]. In addition, indicating that each pollutant is influenced in a different way by altitude due to their chemical composition, reaction properties, disintegration and diffusion over long or short distances [29]. This statement validates our earlier discussion that lower altitudes favors  $\text{PM}_{10}$  distribution while higher altitudes favor  $\text{NO}_2$  and  $\text{SO}_2$  distribution. Interestingly, relative humidity in Fig. 4(a) showed an inverse relationship to wind speed as previously observed [31] in characterization studies of criteria air pollutants. Guo and co-workers reported that Southerly low speed winds and high relative humidity permits the buildup of pollutants as observed in upper Iweka, while high speed Northerly winds and low relative humidity result in good air quality as detected at C.K.C, Borromeo and Awada sampling areas.



**Fig. 3. GIS plot for (a)  $\text{SO}_2$ , (b)  $\text{NO}_2$ , and (c)  $\text{PM}_{10}$  for Onitsha Lower Basin at Point 1**



**Fig. 4. Effect of (a) relative humidity, (b) Elevation, (c) wind speed, (d) Temperature on SO<sub>2</sub> concentration at Onitsha points 1**

Then again, Fig. 4(c) depicts the effect of wind speed over SO<sub>2</sub> at point 1. It shows that the high convention of wind operates on Fegge/Nupe square and CKC and influences SO<sub>2</sub> and NO<sub>2</sub> distribution. This relationship was earlier observed during Spatio-temporal discussion on this article and correlates with similar study [14] done on appraisal of spatio-temporal variants in the air quality of Jaipur city, India. Furthermore, this observed patterns of SO<sub>2</sub> and NO<sub>2</sub> pattern of distribution shows that lesser NO<sub>2</sub> distribution at Fegge/Nupe square and lesser SO<sub>2</sub> distribution at C.K.C are largely due to prevalent high wind speeds.

On the contrary, Upper Iweka has the least of windspeed and encourages the settling of pollutants especially SO<sub>2</sub> and NO<sub>2</sub>. Finally, the measured temperature at Fig. 4(d) showed that the maximum temperature was around 39.5 °C at mission road and minimum at 26 °C at Borromeo hospital. Temperature parameter in Fig. 4(d) showed no interactive behavior against the measured pollutant. However, the temperature parameter had an inverse co-relationship with relative humidity in Fig. 4(a). Hence the two graphs affirm that when relative humidity is high it is usually accompanied by lower temperature

while low relative humidity is accompanied by high temperature. This study thus validates the already existing meteorological knowledge of relative humidity, precipitation and temperature. Because at 70 % being the highest measured relative humidity, the air is saturated and likely to rain or precipitate which afterwards drives colder air and consequent decrease in temperature. This result had also been observed by author who studied the effect of temperature and relative humidity on rainfall [32].

### 3.4 Air Quality Index (AQI) Relationship

Using box central plot from Origin Pro 9.0, the air quality index for Onitsha lower basins during Harmattan of 2014 and 2015 is represented in Fig. 5. The air quality index is categorized into 7 sub divisions representing Good, Moderate, Sensitive, Unhealthy, very unhealthy and hazardous 1 and hazardous 2 as represented on the vertical axis of the right hand side. Each category is assigned a color for significance and identification. The central vertical line represents the numerical grades/range for each AQI category. The cut-off point concentration of air pollutants is also found in US EPA [33].

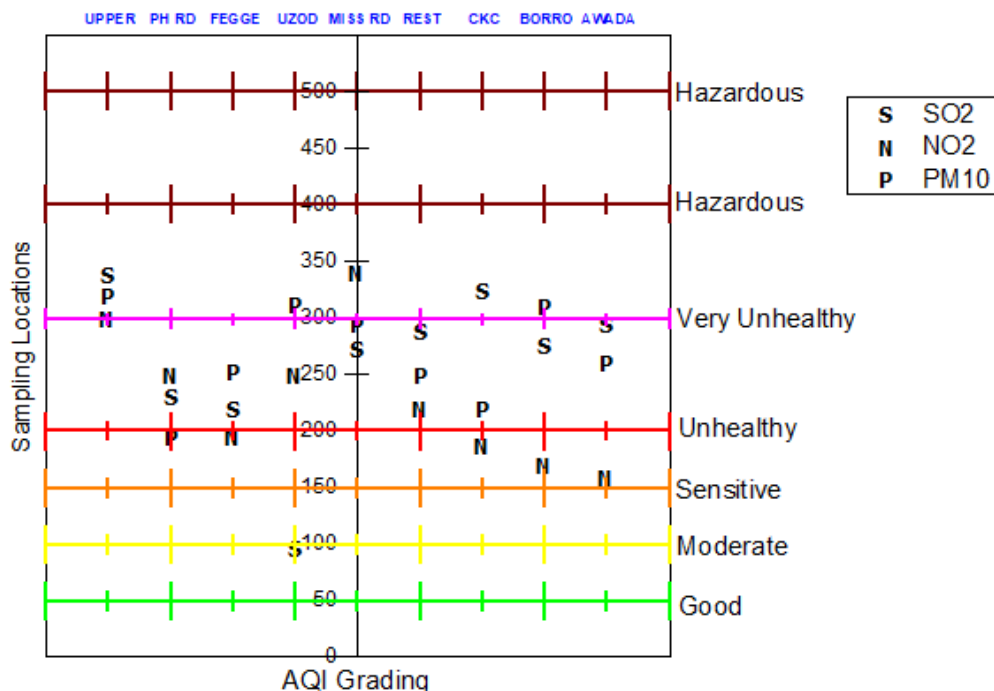


**Fig. 5. Air quality index expressed in scatter central plot**

The sampled locations are shown on the horizontal lines intersected by vertical lines of each AQI category. Their respective location titles are shown at the intersections of the horizontal line. Also, the three criteria pollutants in the box central plot are represented by their first letters. The AQI results were interpolated and calculated for a period of Harmattan of the 2014 and 2015 season. A detailed observation shows that no sampled area falls within AQI good category as well as hazardous category 2. This means that all sampled areas had AQI above 50 and below 400; hence, SO<sub>2</sub>, NO<sub>2</sub>, and PM<sub>10</sub> are principal pollutants in Onitsha lower basin [6]. Many of the sampled areas were within unhealthy, very unhealthy and hazardous category 1 for both gaseous and particulate pollutants. This falls within the health alert category where the urban dwellers may experience health effects and greater likelihood to affect the entire populations' health.

The levels of nitrogen at Awada, Borromeo and CKC (at higher elevation) was calculated to be 159, 170 and 187 and hence the presence of NO<sub>2</sub> using AQI (though lower value) is deemed unhealthy when compared to other sampling areas at lower elevations with higher measured value. This also agrees that higher urban altitude creates an inhibitory effect on urban AQI [30].

Furthermore, the AQI revealed that NO<sub>2</sub> was the primary pollutant at Mission road and pH road for these sampled locations. Likewise SO<sub>2</sub> was prime pollutants at Upper Iweka, Rest house, C.K.C and Awada, while particulate matters (PM<sub>10</sub>) were the principal pollutants at Fegge, Uzodinma and Borromeo in these sampled locations. Hence, the spatio-temporal distribution of air quality index (AQI) evidently represents severe air pollution in Onitsha Lower basin during Harmattan of 2014 and 2015 season.

#### 4. CONCLUSION

From the research findings, Borromeo area and Fegge presented the lowest dip in SO<sub>2</sub> concentration due to prevalent high winds and precipitation, while NO<sub>2</sub> pollutant is dominant and dynamic in Upper Iweka than other regions. Nevertheless, point 3 showed the highest PM<sub>10</sub> distribution and indicated PM<sub>10</sub> is the major pollutant exerting the most significant influence on air quality in the Onitsha Lower basin. Likewise, the behavior of SO<sub>2</sub> and NO<sub>2</sub> are encouraging the formation of PM<sub>10</sub> pollutants within the same region. Conversely, spatial distribution of SO<sub>2</sub> shows that Rest house, Mission road, Fegge/NUPE square, Borromeo and CKC sampling locations were affected by meteorological conditions. Moreover the PM<sub>10</sub>

GIS plot in Fig.3(c) had Upper Iweka, PH road as significantly active region amid PM<sub>10</sub> pollutants spreading out from these sampling areas. Furthermore, meteorological influence shows that the high convention of wind operates around Fegge/Nupe square and CKC and influences SO<sub>2</sub> and NO<sub>2</sub> distribution. At the same time, lower altitudes favor PM<sub>10</sub> circulation and higher altitudes favor NO<sub>2</sub> and SO<sub>2</sub> distribution, while higher urban elevations create inhibitory effects on urban AQI. In conclusion, the study identified SO<sub>2</sub>, NO<sub>2</sub>, and PM<sub>10</sub> as primary pollutants of the Onitsha lower basin. Consequently, the levels of SO<sub>2</sub>, NO<sub>2</sub> and PM<sub>10</sub> have the potential to adversely affect air quality across the studied nine locations subject to meteorological influence. Hence, the recommendation is that baseline monitoring operations are set up and made functional. This will utilize information obtained from spatio-temporal studies, find geographical hot spots, peak concentration areas and episodes, and live public information systems on pollution alerts.

## COMPETING INTERESTS

Authors have declared that no competing interests exist.

## REFERENCES

1. Babayemi J, Ogundiran MB, Osibanjo O. Overview of environmental hazards and health effects of pollution in developing countries: a case study of Nigeria. *Environ. Qual. Manage.* 2017;26(1):51-71. Available:<https://doi.org/10.1002/tqem.21480>
2. Ityavyar EM, Thomas TT. Environmental pollution in Nigeria: The need for awareness creation for sustainable development. *J. Res. For. Wildl. Environ.* 2012;4(2):1-14
3. Marlier ME, Jina AS, Kinney P.L. Extreme Air pollution in global megacities. *Curr. Clim. Change. Rep.*, 2016;2:15-27. Available:<https://doi.org/10.1007/s40641-016-0032-z>
4. Cunningham A. Amid Pollution and political indifference, Nigerians struggle to catch their breath. (Accessed: 19 November 2019) Available:<https://undark.org/2018/10/22/air-pollution-lagos/#>
5. Utang PB, Peterside KS. Spatio-temporal variations in urban vehicular emission in Port Harcourt city, Nigeria. *Ethiop. J. Environ. Stud. Manage.* 2011;4(2):38-51 Available:<https://doi.org/10.1007/s40641-016-0032-z>
6. Anyika LC, Alisa CO, Nkwoada AU, Opara AI, Ejike EN, Onuoha GN. GIS and MATLAB modeling of criteria pollutants: A study of lower Onitsha basin during rains. *J. Sci. Technol. Environ. Inform.* 2018;6(1):443-457. Available:<https://doi.org/10.18801/jstei.060118.47>
7. Nkwoada A, Oguzie E, Alisa C, Agwaramgbo L, Enenebeaku C. Emissions of gasoline combustion by products in automotive exhausts. *Int. J. Sci. Res. Publ.* 2016;6(4):464-482.
8. Azadi H, Verheijke G, Witlox F. Pollute first, clean up later? *Global. Planet. Change.* 2011;78(3/4):77-82. Available:<https://doi.org/10.1016/j.gloplach.2011.05.006>
9. Buckland K, Young S, Keim E, Johnson R, Johnson P, Tratt D. Tracking and quantification of gaseous chemical plumes from anthropogenic emission sources within the Los Angeles Basin. *Remote. Sens. Environ.* 2017;201:275-296. Available:<https://doi.org/10.1016/j.rse.2017.09.012>
10. Bakri NMN, Al-Junid MAS, Razak AHA., Idros MFM, Halim KA. Mobile carbon monoxide monitoring system based on arduino-matlab for environmental monitoring application. paper presented at the 4th international conference on electronic devices, systems and applications (ICEDSA) 14-15 September 2015. IOP Publishing IOP Conf. Series: Materials Science and Engineering. 2015;99:012009. Available:<https://doi.org/10.1088/1757-899x/99/1/012009>
11. Said M, Safwat G, Turki M, Mamoun A. Spatiotemporal analysis of fine particulate matter (PM2.5) in Saudi Arabia using remote sensing data. *Egypt. J. Remote Sens. Space Sci.* 2016;19(2):195-205. Available:<https://doi.org/10.1016/j.ejrs.2016.06.001>
12. Zhao L, Meihui X, Kun T, Peichao G. GIS-based analysis of population exposure to PM2.5 air pollution: A case study of Beijing. *J. Environ. Sci.* 2017;59:48-53. Available:<https://doi.org/10.1016/j.jes.2017.02.013>

13. Fatehifar EA, Elkamel A, Taheri M. A MATLAB-Based modeling and simulation program for dispersion of multipollutants from an industrial stack for educational use in a course on air pollution control. *Comp. Appl. Eng. Edu.* 2006;14(4):300-312. Available:<https://doi.org/10.1002/cae.20089>
14. Ankita P, Rohit G, Pran N. Assessment of spatio-temporal variations in air quality of Jaipur city, Rajasthan, India. *The Egypt. J. Remote Sensing Space Sci.* 2018;21(2):173-181. Available:<https://doi.org/10.1016/j.ejrs.2017.04.002>
15. Wang Y, Ying Q, Hu J, Zhang H. Spatial and temporal variations of six criteria air pollutants in 31 provincial capital cities in China during 2013–2014. *Environ.* 2014;73:413-422. Available:<https://doi.org/10.1016/j.envint.2014.08.016>
16. Dong R, Youping L, Hong Z, Xiaoxia Y, Xiaoman L, Xuejun P, Bin H. Spatiotemporal variations and possible sources of ambient pm10 from 2003 to 2012 in Luzhou, China. *Environ. Eng. Res.* 2015;19(4):331-338. Available:<https://doi.org/10.4491/eer.2014.038>
17. Maurya PS, Yadav KA. Evaluation of course change detection of Ramganga river using remote sensing and GIS, India. *Weather Clim. Extremes.* 2016;13:68-72. Available:<https://doi.org/10.1016/j.wace.2016.08.001>
18. Fatehifar E, Elkamel A, Osalu A.A. Charchi A. Developing a new model for Simulation of pollution dispersion from a network of stacks. *App. Math. Comput.* 2008;206(2):662-668. Available:<https://doi.org/10.1016/j.amc.2008.05.120>
19. Chen W, Yan L, Zhao H. Seasonal Variations of Atmospheric Pollution and Air Quality in Beijing. *Atmos.* 2015;6:1753-1770. Available:<https://doi.org/10.3390/atmos6111753>
20. FEPA. Federal environmental protection agency act 1: National effluent limitations and gaseous emissions guidelines in Nigeria for specific industries; 1991. Available:<http://lawsfnigeria.placng.org/laws/F10.pdf> (Accessed: 18 September 2019)
21. Tecer LH, Tagil S. Spatial-temporal variations of sulphur dioxide concentration, source, and probability assessment using a gis-based geostatistical approach. *Pol. J. Environ. Stud.* 2013;22(5):1491-1498.
22. Subrata C, Srimanta G, Raj NS. Spatial and temporal variation of urban air quality: A GIS Approach. *J. Environ. Prot.* 2010;1:264-277.
23. Hong G, Xingfa G, Guoxia M, Shuaiyi S, Wannan W, Xin Z, Xiaochuan Z. Spatial and temporal variations of air quality and six air pollutants in China during 2015–2017. *Nature Res. Sci. Rep.* 2019;9(15201)1-7. Available:<https://doi.org/10.1038/s41598-019-50655-6>
24. Velders GJN, Geilenkirchen GP, De-Lange R. Higher than expected NOx emissions from trucks may affect attainability of NO<sub>2</sub> limit values in the Netherlands. *Atmos. Environ.* 2011;45(18):3025-3033. Available:<https://doi.org/10.1016/j.atmosenv.2011.03.023>
25. Tian D, Fan J, Jin H, Mao H, Geng D, Hou S, Zhag P, Zhang Y. Characteristic and spatiotemporal variation of air pollution in Northern China based on correlation analysis and clustering analysis of five air pollutants. *JGR Atmos.* 2020;125(8)1:1-8. Available:<https://doi.org/10.1029/2019jd031931>
26. Dey S, Gupta S, Sibanda P, Chakraborty, A. spatio-temporal variation and futuristic emission scenario of ambient nitrogen dioxide over an urban area of Eastern India using GIS and coupled AERMOD-WRF Model. *PLoSOne.* 2017;12(1):e0170928. Available:<https://doi.org/10.1371/journal.pone.0170928>
27. WHO. WHO air quality guidelines for particulate matter, ozone, nitrogen dioxide and sulfur dioxide; 2005. Available:[http://apps.who.int/iris/bitstream/10665/69477/1/WHO\\_SDE\\_PHE\\_OEH\\_06.02\\_eng.pdf](http://apps.who.int/iris/bitstream/10665/69477/1/WHO_SDE_PHE_OEH_06.02_eng.pdf). (Accessed: 17 November 2019)
28. Sahu V, Gurjar BR. Spatio-temporal variations of indoor air quality in a university library. *Int. J. Environ. Health Res.* 2019;1:1-16. Available:<https://doi.org/10.1080/09603123.2019.1668916>
29. Sharma M, Pal B, Pal A, Bajpai AB. Spatio-temporal changes and impact of air

- pollution on human health: A case study of Dehradun City. *Essence Int. J. Environ. Rehab. Conserv.* 2017;7(1):1-10.
30. Sun Z, Zhan D, Jin F. Spatio-temporal characteristics and geographical determinants of air quality in cities at the prefecture level and Above in China. *Chin. Geogra. Sci.* 2019;29(2):316-324.  
Available:<https://doi.org/10.1007/s11769-019-1031-5>.
31. Guo H, Wang Y, Zhang H. Characterization of criteria air pollutants in Beijing during 2014–2015. *Environ. Res.* 2017;154:334-344.
32. Available:<https://doi.org/10.1016/j.envres.2017.01.029>
33. Mawonike R, Mandonga G. The effect of temperature and relative humidity on rainfall in Gokwe region, Zimbabwe: A factorial design perspective. *Int. J. Multidiscip. Acad. Res.* 2017;5(2):36-46.
- US EPA. Guideline for reporting of daily air quality—Air quality index (AQI) (EPA-454/R-99-010). Office of Air Quality Planning and Standards;1999.  
Available:[https://www.epa.gov/sites/production/files/2017-1/documents/trends\\_report\\_2003.pdf](https://www.epa.gov/sites/production/files/2017-1/documents/trends_report_2003.pdf)  
(Accessed: 7 February 2020)

© 2020 Anyika et al.; This is an Open Access article distributed under the terms of the Creative Commons Attribution License (<http://creativecommons.org/licenses/by/4.0>), which permits unrestricted use, distribution, and reproduction in any medium, provided the original work is properly cited.

**Peer-review history:**

The peer review history for this paper can be accessed here:  
<http://www.sdiarticle4.com/review-history/59196>